



Survey and Classification of Soil Texture on both Banks of Sirwan River, Kurdistan Region, Iraq Using Remote Sensing and GIS.

Salim Neimat Azeez

Protected Cultivation Department, Bakrajo Technical Institute, Sulaimani Polytechnic University, Sulaymaniyah, Iraq.

Email: salim.azeez@spu.edu.iq

Abstract:

This study uses integrated remote sensing (RS) and geographic information system (GIS) methods to analyze the survey and classification of soil texture on both sides of the Sirwan River. The main problem of this study is that there is no accurate description of the soil texture of the study area through GIS. The study region, which spans 79.7 km between Darbandikhan and Kalar in the Kurdistan Region of Iraq, was examined using field sampling and laboratory analysis of 30 soil sites. Using the United States Department of Agriculture (USDA) Soil Texture Triangle, soil texture was classified according to the ratios of sand, silt, and clay. Spatial modeling in ArcMap was supported by Landsat 9 satellite imagery. The main objectives of this study is to classify soil texture, to show the impact of fluvial dynamics on the difference in soil textures between the two river banks and to mapping soil texture of the study area. The results showed that the region's major soil textures are loamy (66.5%) and silty loam (33.5%), which are caused by the river's fluvial environment's sediment deposition patterns. Because of continuous quarrying operations, the left riverbank displayed more variation in soil particle distribution, whereas the right bank was more stable. The sediment sorting process was confirmed by statistical analysis, which revealed significant correlations between soil elements. The combination of remote sensing and geographic information systems proved useful for mapping soil heterogeneity and provided significant information for land use planning, erosion control, and sustainable agriculture. The study emphasizes the promise of digital soil mapping methods and suggests further investigation of unmanned aerial vehicles (UAVs) and hyperspectral imaging to improve accuracy.

Keywords: Survey and Classification, Sirwan River, Kurdistan Region, Geographic Information System, Remote Sensing.

المخلص:

تستخدم هذه الدراسة أساليب الاستشعار عن بُعد المتكاملة ونظم المعلومات الجغرافية لتحليل وتصنيف نسيج التربة على ضفتي نهر سيروان. تكمن المشكلة الرئيسية لهذه الدراسة في عدم وجود وصف دقيق لنسيج التربة في منطقة الدراسة باستخدام نظم المعلومات الجغرافية. وقد تم فحص منطقة الدراسة، التي تمتد على مسافة 79.7 كيلومتراً بين دربندخان وكلا في إقليم كردستان العراق، باستخدام أخذ عينات ميدانية وتحليل مختبري لـ 30 موقعاً للتربة. وباستخدام مثلث نسيج التربة التابع لوزارة الزراعة الأمريكية، تم تصنيف نسيج التربة وفقاً لنسب الرمل والطين والطين. وقد تم دعم النمذجة المكانية في برنامج ArcMap بصور القمر الصناعي Landsat 9. تتمثل الأهداف الرئيسية لهذه الدراسة في تصنيف نسيج التربة، وبيان تأثير ديناميكيات الأنهار على اختلاف نسيج التربة بين ضفتي النهر، ورسم خريطة لنسيج التربة في منطقة الدراسة. أظهرت النتائج أن قوام التربة الرئيسي في المنطقة هو الطيني (66.5%) والطيني الغريني (33.5%)، وهو ما ينتج عن أنماط ترسب الرواسب في البيئة النهرية للنهر. وبسبب عمليات استخراج الأحجار المستمرة، أظهر الضفة اليسرى للنهر تبايناً أكبر في توزيع جزيئات التربة، بينما كانت الضفة اليمنى أكثر استقراراً. وقد تم تأكيد عملية فرز الرواسب من خلال التحليل الإحصائي، الذي كشف عن وجود ارتباطات معنوية بين عناصر التربة. وقد أثبت الجمع بين الاستشعار عن بعد ونظم المعلومات الجغرافية جدواه في رسم خرائط عدم تجانس التربة، ووفر معلومات مهمة لتخطيط استخدام الأراضي، ومكافحة التعرية، والزراعة المستدامة. وتؤكد الدراسة على إمكانات أساليب رسم خرائط التربة الرقمية، وتقترح إجراء المزيد من الأبحاث من خلال استخدام الطائرات بدون طيار والتصوير الطيفي الفائق لتحسين الدقة.

الكلمات المفتاحية: المسح والتصنيف، نهر سيروان، إقليم كردستان، نظم المعلومات الجغرافية، الاستشعار عن بعد.

بوخته:

نم تويژينهويه له تهكنيكهكاني ههستكردن له دورموه و سيستهمي زانباري جوگرافي (GIS) كهلك وهردهگريته بۆ شيركردنهوه و پۆلنكردي پيکهاتهي خاک بهدریزي کهنارهکاني رووباري سيروان. تهعهديهكي سهرمكي لهه ليکولينهويهدها نهپووني وهسفيکي گشتهگيره لهسهه بنهماي GIS بۆ پيکهاتهي خاک له ناچهي ليکولينهويهکهدها. رووباري تويژينهويهکه که 79.7 كيلومتر له نيوان دهرينهديخان و کهلار له ههريمي کوردستاني عيراق دهگريتهموه، به بهکارهيناني سامپلي مهيداني و شيکاري تاقهگيهي 30 شويني خاک پشکيني بۆ کراوه. پيکهاتهي خاکهکه بهپي ريژهي لم، ليته و گل (قور) به بهکارهيناني سيگوشهي پيکهاتهي خاكي USDA پۆلن کرا. مۆدیلکردني شويني له ArcMap به وينه مانگي دهستکردي Landsat 9 پشتهگيري کرا. نامانجه سهه مکيهکاني نم تويژينهويهه بريتهن له پۆلنکردني پيکهاتهي خاک، نيشانداني کاريگري دايناميکي رووبارهکان لهسهه گۆرانکاربيهکاني پيکهاتهي خاک له نيوان کهنارهکاني رووبارهکهدها، و نهخشهکيشاني پيکهاتهي خاک له ناچهي ليکولينهويهکهدها. نهجهمهکان دهرينهدهخن که پيکهاتهي خاكي بالادهست له ناچهکهدها گل (66.5%) و گلن ليتهي (33.5%)، که له نهجهمي شيوازي نيشتهي نيشتهو له ژينگهه کهنارهکاني رووبارهکهدها دروست بووه. بههوي بهردهوامي ههلهگرتي بهرد، کهناري چهپي رووبارهکه گۆرانکاري زياتري له دابهشبووني گهرديلهکاني خاکدا نيشان دا، لهکاتیکدا کهناري راست جيهگيرتر بوو. ريزکردني نيشتهوهکان به شيکاري ناماري پشتهه استکر ايهوه، که پهيوهنديهکي بهرچاوي له نيوان پيکهاتهکاني خاکدا ناشکرا کرد. تیکهلهکردني ههستکردن له دورموه و سيستهمي زانباري جوگرافي (GIS) کاريگهه بوو له نهخشهکيشاني نايهکساني خاک، دابينکردني زانباري بهنرخ بۆ پلانداناني بهکارهيناني زهوي، کۆنترۆلکردني وهريني زهوي و کشتوکالي بهردهوام. نم تويژينهويهه تيشک دهخاته سهه تواناي شيوازهکاني نهخشهسازي ديجيتالي خاک و پيشنياري ليکولينهويهه زياتر دهکات بهکارهيناني فروکهي بيفروکهوان و پنهگرتني هاپيهه سپيکترال بۆ بهزرکردنهوهي وردبيني.

کليه وشه: رووپيوي و پۆلنکردن، رووباري سيروان، ههريمي کوردستان، GIS، ههستکردن له دورموه

1. Introduction

Soil texture is characterized by the relative proportions of sand, silt, and clay within the soil matrix, and it plays a crucial role in controlling properties such as water retention, nutrient availability, and susceptibility to erosion [1]. Soil texture fundamentally governs many soil characteristics that influence agricultural productivity, hydrological behavior, and environmental sustainability [2]. In riverine environments, soil texture profoundly influences sediment transport, floodplain dynamics, and the formation and complexity of aquatic habitats [3]. Understanding the spatial variability of soil texture along river banks is essential for sustainable land management, particularly in areas prone to erosion or intensive agricultural activity. River banks are highly dynamic environments where soil texture can vary markedly due to the deposition of sediments carried by river water. In these zones, the texture is shaped by factors such as flow velocity, sediment particle size, and frequency of flooding [4]. Therefore, understanding the distribution of soil texture is critical for erosion management, sedimentation control, and sustainable land use planning. Fine-textured soils (clay and silt) tend to retain water and nutrients, but are susceptible to compaction and reduced aeration, which can limit plant growth.

Coarse-textured soils such as sands significantly enhance drainage and aeration but often have low nutrient retention and are more prone to erosion [5]. Therefore, knowing how soil texture is distributed spatially is essential for boosting agricultural productivity, limiting environmental degradation, and enhancing the performance of hydrological models [6]. A river basin's hydrological and ecological processes are significantly influenced by its soil texture. Due to their coarse texture, sandy loam allow for quick drainage, which lowers the risk of flooding but restricts the water retention that plants need [7]. Conversely, fine-textured soils, such as clay, enhance moisture retention but are more susceptible to increased runoff and erosion due to their low permeability and cohesive nature [8]. On river banks, the soil texture affects sedimentation patterns, bank stability, and forest vegetation health [9]. For instance, dynamic river flows deposit graded sediments, resulting in heterogeneous soil textures that vary with seasonal flooding cycles [10]. Accurate classification of these textures is therefore critical for predicting erosion zones, improving agricultural practices, and restoring degraded ecosystems. Optical remote sensing methods use spectral indices such as the normalized difference soil index (NDSI) and redness index (RI) to infer soil texture properties [11]. Both Synthetic Aperture Radar (SAR) and micro remote sensing techniques offer valuable insights into soil moisture and texture variations, which are indirectly related to changes in soil texture [12]. Clay-rich soils exhibit distinct spectral signatures due to their high moisture-holding capacity and mineral composition, which influence their reflectance characteristics in the infrared spectrum. [13]. The United States Department of Agriculture (USDA) Soil Texture Triangle, which categorizes soils into 12 textural classes based on their texture, is the most commonly used method for classifying soil texture in terms of the proportion of sand, silt, and clay [14]. Remote sensing (RS) and geographic information systems (GIS) methods enable estimating soil texture proportions by analyzing spectral reflectance patterns that vary according to soil mineral composition and particle size [15]. For instance, clay soils have lower reflectivity due to their smaller particle size and greater moisture retention, whereas sandy soils have higher reflectivity in the visible and near-infrared wavelengths [16]. By taking advantage of these spectral differences, researchers can develop predictive models to

estimate soil texture and classify it according to standard textural categories. The study of soil texture along river banks using remote sensing and GIS techniques is of great importance for environmental management and sustainable development. River banks are ecologically sensitive areas that provide habitats for a wide variety of plants and animals, and their soil properties are crucial for maintaining ecosystem health [17].

In recent years, RS and GIS have emerged as powerful tools for large-scale soil texture mapping and classification, providing cost-effective and more efficient alternatives to traditional methods. To illustrate, the possibility of utilizing spectral reflectance data from satellite imagery to forecast soil texture, highlighting the link between soil attributes and spectral signatures [13]. These techniques enable efficient spatial analysis of soil properties across diverse landscapes, opening up new avenues for natural resource management. [18] Recent studies have utilized GIS-based spatial interpolation techniques to map soil texture distribution in river basins, effectively integrating remote sensing data with topographic and environmental variables to enhance prediction accuracy. These studies underscore the importance of combining RS and GIS techniques to achieve accurate and effective soil texture classification. RS and GIS provide an effective framework for soil texture mapping and classification in these environments, enabling researchers and land managers to make informed decisions.

Recent studies have demonstrated the effectiveness of RS and GIS in soil texture mapping. [19] For instance, Landsat satellite imagery combined with topographic features has been utilized to predict soil texture in river basins in Brazil, achieving accuracies up to 85%. [20] used Sentinel-2 satellite data and machine learning techniques to classify soil texture in the Yellow River Basin in China, highlighting the role of the NDVI in reducing the influence of vegetation interference on the classification. Other studies have also demonstrated the potential of remote sensing and GIS in soil texture mapping. GIS facilitate the analysis of spatial relationships between soil texture and various environmental factors, such as topography, land use, and hydrology, thereby providing valuable insights for natural resource management [21]. Despite the benefits of remote sensing and GIS, there are obstacles to their application in soil texture mapping. The difficulty of acquiring high-resolution soil information for validating and calibrating models [13]. Other variables that might influence the correctness of soil texture forecasts include vegetation cover, soil moisture, and weather circumstances, all of which can mask spectral signatures [15]. In order to address these challenges, researchers are integrating field data, laboratory results, and remote sensing data from soil samples to produce high-resolution soil texture maps. [18].

Research objectives:

This research aims to utilize these techniques to study and classify soil texture along river banks, providing important insights into geomorphological processes and land use planning. This research explores the integration of RS and GIS techniques in classifying soil texture along river banks, filling gaps in river soil maps and contributing to informed land use decisions by:

1. Classify soil texture on both banks of a river using RS and GIS.
2. Evaluate the impact of fluvial dynamics on textural spatial variability.
3. Analyze soil texture distribution by integrating remote sensing imagery with field-based data.

4. Provide decision-makers with valuable insights for sustainable agriculture, environmental management, and resource conservation.

2. Study area

The study area is located along the banks of the Sirwan River between the cities of Darbandikhan and Kalar (Figure 1), with a length of 79.7 km, the soil samples were taken from both river banks. The distance between the points is 6.5 km, with area of 160 km². The study area is between longitudes 45° 14' 34.22" E and 45° 42' 02.82" E and latitudes 34° 31' 23.58" N and 35° 50' 12.5" N (Figure 1). The northern part of the study area is located within the Zagros Mountains, and the southern part is located within the foothills [22]. The climate is influenced by the steppe climate, which is continental semi-arid PE (Potential Evapotranspiration) [23]. The soils of the study area belong to the Aridisols and Mollisols Orders [24, 25 and 26]. The soil temperature regime is Hyperthermic [27], while the soil moisture regime is Toric [28]. There is a significant variation in climatic elements between the north and south of the study area, where the rainfall rate in the north of the study area is 726.8 mm and an average temperature of 22.46 °C (Darbandikhan Dam weather station), while in the south of the study area the rainfall rate is 286.8 mm with average temperature of 25.10 °C (Kalar weather station). Rainfall is seasonal, as it falls in winter, spring and autumn and does not fall in summer [28]. It is important to mention that the crops and wild plants seen in the research area serve as indicators during the survey of the study region. Some parts are used for farming such as vegetables and orchards, while other baren lands still have various native plants like wild barley (*Hordeum spontaneum*), Bermuda grass (*Cynodon dactylon*) and wild reed (*Phragmites australis*) [29].

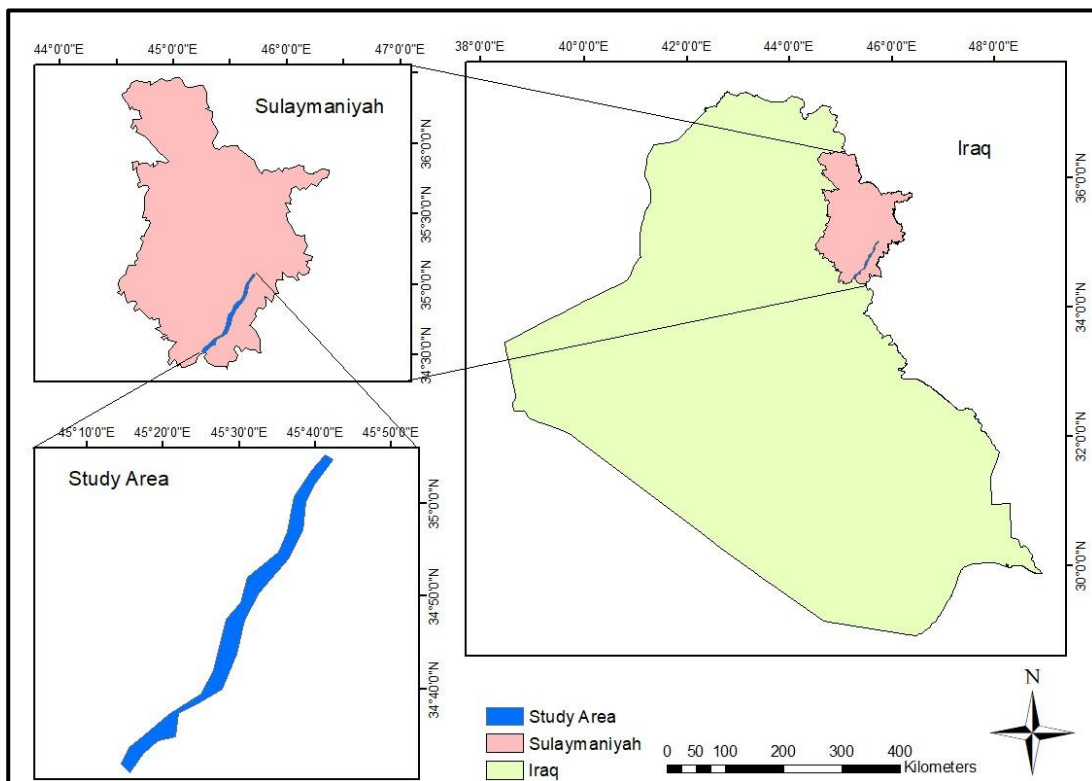


Figure 1: The study area [Author]

3. Materials and Methods

This research relied on an integrated approach that combined field data collection from soil surveys, spatial data, and soil samples from the study area, remote sensing analysis, and GIS-based spatial modeling to classify soil texture along the banks of the Sirwan River. Soil texture distribution and classification maps were produced using ArcMap software from satellite imagery and Basemap maps (Figure 2).

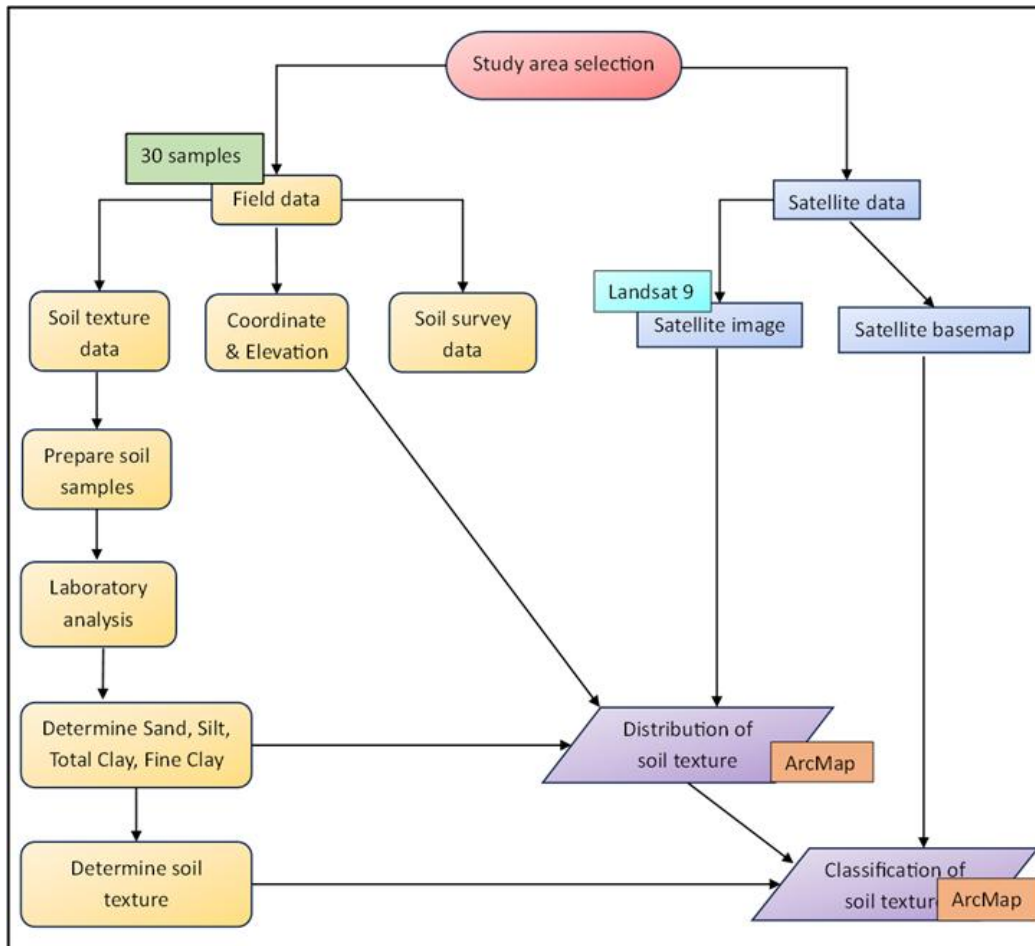


Figure 2: Frame work of the study [Author]

3.1. Data Used

At the beginning, the location was selected, then a topographic map [30] and a reconnaissance soil survey map prepared by [31] were used as basic maps for this study. The soil order, type of vegetation cover, and rock condition of the study area were detected. The data included two types: the first, concerning field data, was a total of 30 locations on the topographic map, 6.5 km apart distance between each other were selected using a grid system method. The soil samples were taken from the locations within 30 cm depth from the soil surface. A morphological description was conducted according to [32]. Soil samples were air dried and mixed to be homogenous, grinded using a wooden mortar, then passed through a 2 mm sieve and kept in plastic containers for further analyses. Particle size was determined by using the International Pipette Method as described in [33]. The silt and clay were separated from sand by washing the dispersed samples through a 50 µm sieve, as

described in [34]. The various silt and clay fractions were thus obtained by the pipette method as described in [35]. The fine clay determined according to [36]. Finally, the soil texture type was determined based on the soil texture triangle [37]. The second used dataset is Landsat 9 Level-1TP (Precision and Terrain) Path-168, Row-036 which is provided by the United States Geological Survey (USGS); taken, in 14th July 2023; vegetation cover was rare in the study area. The Landsat 9 encompasses 11 bands, including Visible, Red, Near-Infrared, Short Wavelength Infrared (SWIR), Panchromatic (PAN), Cirrus and Thermal Infrared Sensor (TIRS), (Table 1) [38].

Table 1: The band, name, wavelength and resolution of Landsat 9 [38].

Band	Name	Wavelength (µm)	Resolution (m)
Band 1	Visible Coastal Aerosol	0.43 - 0.45	30
Band 2	Visible Blue	0.45 - 0.51	30
Band 3	Visible Green	0.53 - 0.59	30
Band 4	Red	0.64 - 0.67	30
Band 5	Near-Infrared	0.85 - 0.88	30
Band 6	SWIR 1	1.57 - 1.65	30
Band 7	SWIR 2	2.11 - 2.29	30
Band 8	Panchromatic (PAN)	0.50 - 0.68	15
Band 9	Cirrus	1.36 - 1.38	30
Band 10	TIRS 1	10.6 - 11.19	100
Band 11	TIRS 2	11.5 - 12.51	100

3.2. Processing

The process included three main steps; the first step related to field data such as surveying the study area and taking coordinates and elevation of soil samples as well as laboratory data for soil samples. The second step is statistical data which shows the relationship between the different soil particles on the two banks of the river, each bank separately. The statistical relationships between the two banks of the river were compared to highlight which two banks are more consistent in the movement of soil particles and the consistency of the relationship between them. The third step is the distribution and classification of soil particles and texture on the two banks of the river, each bank separately, through ArcMap.

3.2.1. Laboratory Analyses

During the laboratory work, sand, silt, clay, fine clay, total clay and fine clay/total clay were determined and the soil texture was selected based on the soil texture triangle according to the locations from which soil samples were taken in the study area, based on the site coordinates (Table 2, a and b).

Table 2, a: Soil texture parameters (Left bank) [Author]

No.	Longitude (E) m	Latitude (N) m	Elevation (m)	Soil particles (g/kg soil)				Fine Clay/ Total Clay	Soil Texture
				Sand	Silt	Total Clay	Fine Clay		
1	562557.04	3882894.20	464	318.41	463.79	217.8	104.03	0.478	L
2	560172.30	3879880.10	450	320.5	470.39	209.11	100.05	0.478	L
3	556767.50	3874750.09	426	314.35	463.72	221.93	88.17	0.397	L
4	555414.11	3868077.07	340	406.31	426.2	167.49	69	0.412	L
5	553619.21	3863915.60	325	512.44	400.18	87.38	34.52	0.395	L
6	547741.33	3858684.00	342	426	455.08	118.92	51.47	0.433	L
7	546071.27	3853718.44	313	191.27	542.41	266.32	143.84	0.540	SiL
8	543507.81	3850482.07	311	380.24	483.72	136.04	57.31	0.421	L
9	542207.51	3846596.14	287	281.13	557.51	161.36	88.19	0.547	SiL
10	540729.22	3840163.91	271	300.19	546.39	153.42	94.93	0.619	SiL
11	538232.31	3835917.58	270	280.17	499.16	220.67	110.39	0.500	L
12	531733.23	3831432.16	208	309.44	496.5	194.06	64.33	0.331	L
13	526839.92	3826934.78	199	323.38	494.16	182.46	55.03	0.302	L
14	523886.37	3824495.24	193	361.19	498.81	140	35	0.250	L
15	522287.13	3821656.41	180	404.2	480.79	115.01	28.53	0.248	L

Table 2, b: Soil texture parameters (Right bank) [Author]

No.	Longitude (E) m	Latitude (N) m	Elevation (m)	Soil particles (g/kg soil)				Fine Clay/ Total Clay	Soil Texture
				Sand	Silt	Total Clay	Fine Clay		
1	563880.49	3881968.40	465	331.38	441.8	226.82	109	0.481	L
2	559912.07	3876808.63	478	352.15	470.83	177.02	54.44	0.308	L
3	558589.32	3873236.11	430	337	465.69	197.31	86.43	0.438	L
4	557795.57	3867812.00	364	365.58	486.33	148.09	45.53	0.307	L
5	554990.29	3862510.08	315	319.22	477.52	203.26	71.43	0.351	L
6	549153.95	3855508.48	292	200.81	546.72	252.47	117.54	0.466	SiL
7	546285.80	3849953.27	278	291.13	562.51	146.36	61.19	0.418	SiL
8	544698.00	3843338.17	277	305.77	562.02	132.21	56.14	0.425	SiL
9	541806.20	3836204.55	253	289.25	551.42	159.33	74	0.464	SiL
10	536591.72	3833297.28	218	275.36	499.73	224.91	90.3	0.401	L
11	533285.19	3831394.10	236	330.7	469	200.3	31.4	0.157	L
12	532579.39	3827154.16	215	320.4	461.39	218.21	50.85	0.233	L
13	529167.00	3826149.04	201	339.9	460.19	199.91	44.04	0.220	L
14	526321.36	3823511.62	188	371.62	477.38	151	32.11	0.213	L
15	523487.05	3820198.45	178	394.07	466.17	139.76	29.87	0.214	L

3.2.2. Satellite Analysis

The work was carried out in two directions: the first is distributing soil samples on both banks of the Sirwan River on the satellite image to facilitate the process of interpreting the difference in the quantities of fine soil particles and changing their paths. The second is classifying soil particles to know the classes of soil texture present and distributing them on the map of the study area, with calculating the area of each class.

4. Result and Discussion

4.1. Soil Survey

The results indicated that two soil families were identified in the study region (Figure 3). The two families representing the most intensive families area were chosen for the reconnaissance study include the following families: Loamy, mixed, hyperthermic, superactive, calcareous Typic Calciargids which is belongs to Aridisols soil order and Fine loamy, smectitic , hyperthermic, superactive, calcareous Torrertic Calciustolls which is belongs to Mollisils soil order. These results showed that all soils in the study area represent developed soils. In general, the category of soil families and their pattern of distribution within each region reflected the effect of climate, parent material, topographic location and to some extent to the variation of vegetation.

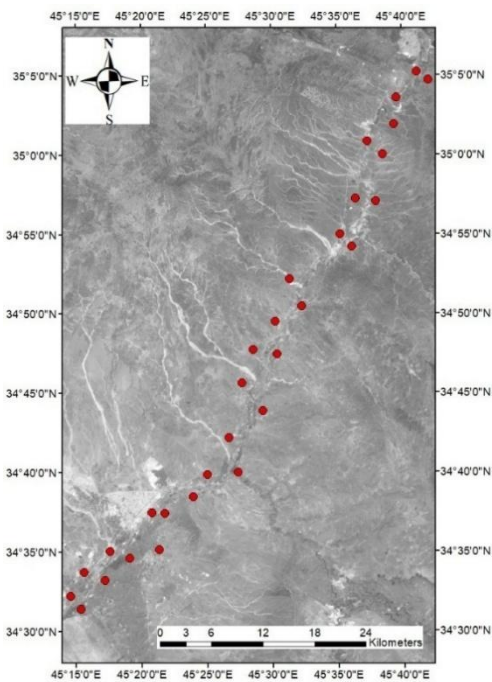


Figure 3: Distribution of soil sample (by using samples coordinates in ArcMap) [Author]

4.2. Soil Particles Classification

Through the results of mechanical analysis of soil particles, it was shown that most of the soil particles on the left bank of the river are located within the silt (Figure 4). As for the right bank, the majority of the soil particles are also located within the silt, but they tend more towards the silty loam (Figure 5). In general, the soil particles on both banks of the Sirwan River are located within the silt. This is due to the nature of the river, which deposits its sediments gradually, as the heavier and coarser sand particles are deposited far from the river course, after that, the silt and then the clay are gradually deposited towards the river. Therefore, it is noted that medium-sized and medium-weight soil particles are prevalent on the river banks, which are more silty with a little bit of clay. It is worth noting, from (Figures 4 and 5), that the soil particles on the right bank are more homogeneous and closer to each other in quantity compared to the left bank. This is due to the nature of the left bank, in which the path of the river changes continuously during the year due to the presence of gravel and sand quarries, which carry out the works of excavation and transport soil materials, which affects the instability and heterogeneity of the soil particles and thus changes the soil texture.

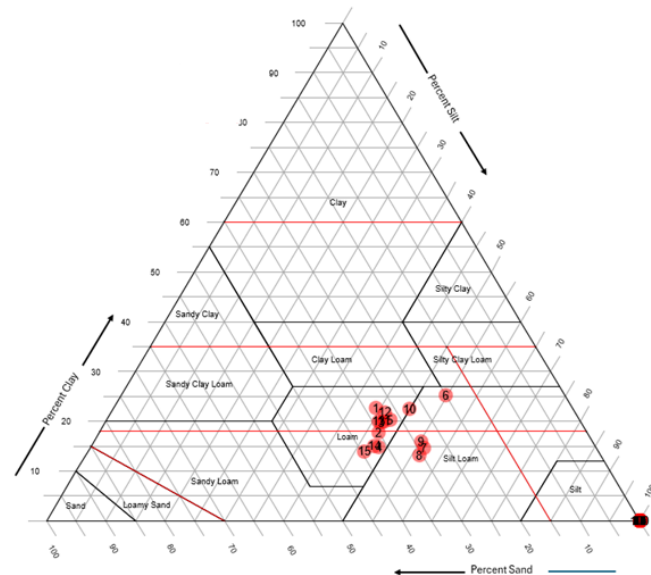
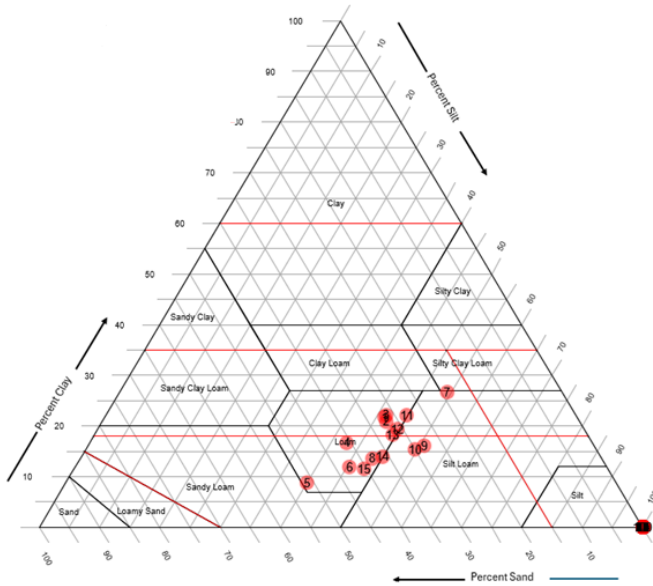


Figure 4: Soil particles texture in (Left Side) [Author] Figure 5: Soil particles texture in (Right Side) [Author]

The soil particle classification maps obtained through ArcMap (Figure 6), indicate that sand class 451-513 (Very High) is generally concentrated at the beginning of the river, while class 191-250 (Very Low) is concentrated in the middle of the study area, and class 321-385 (Moderate) is concentrated at the ends of the river. As for the silt, the 531-563 (Very High) class is concentrated in the middle, and the 400-430 (Very Low) class is found in the northern area near the center of the study area, the medium class 466-500 (Moderate) is generally found at both ends of the river, especially in the southern end. As for the total clay, the 231-267 (Very High) class is in the middle of the study area, while the 87-125 (Very Low) class is concentrated in the middle of the river, the Low, Moderate and High classes may be overlapping in their presence along the river. As for the fine clay, the 121-144 (Very High) class is concentrated in the middle of the study area, while the 28-50 (Very Low) class is mainly concentrated in the southern end of the river, with a small area in the areas near the middle. As for the 76-100 (Moderate) class, it is overlapping along the study area.

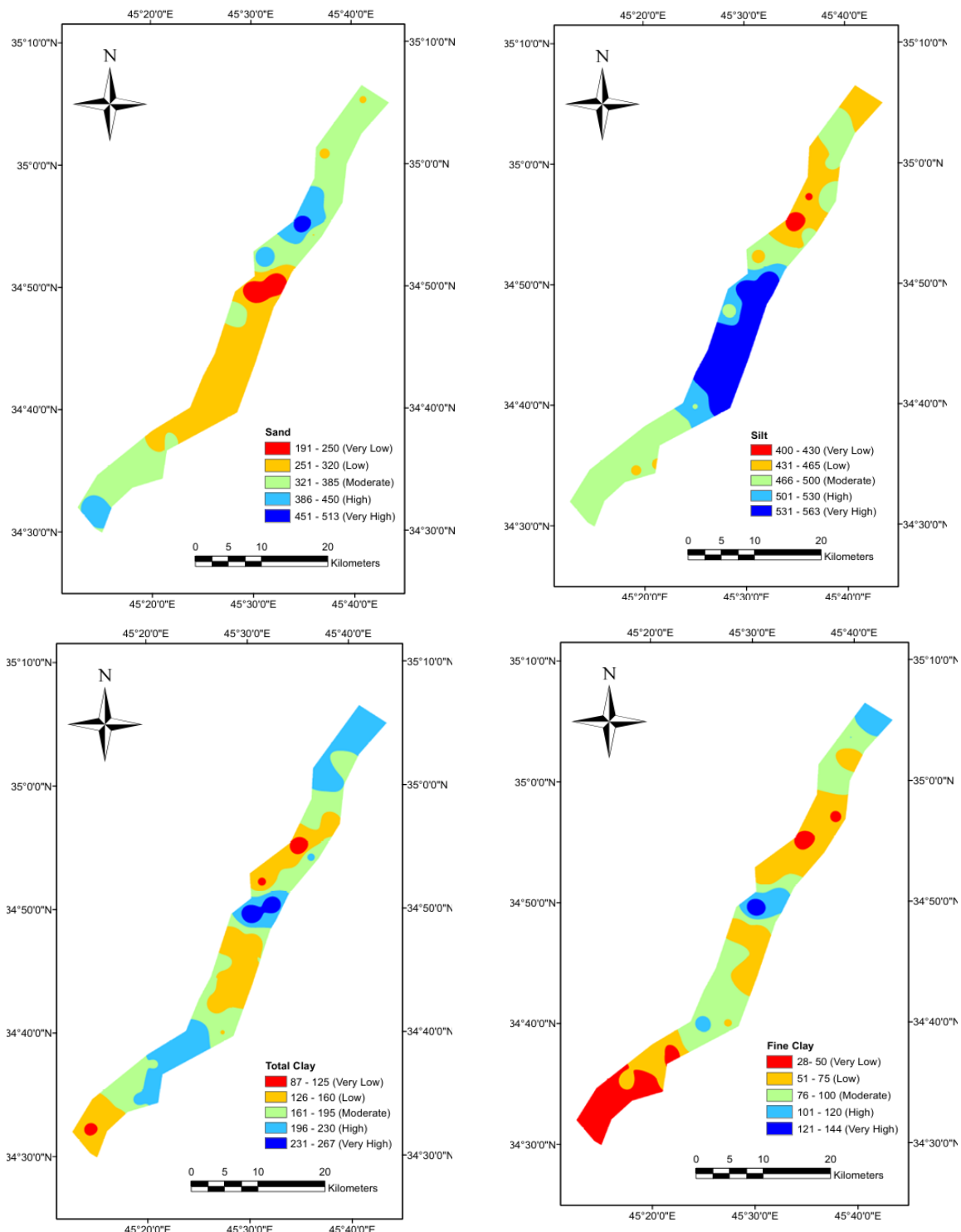


Figure 6: Classification of soil particles [Author]

In general, and through (Figure 7), it is clear that there are no complete coordination and homogeneity between the distribution of the quantities of different soil particles and the river elevation. There is fluctuation in the quantities of soil particles along the river, and an overlap between them is also observed. The reason for this is due to the nature of the Sirwan River, which is greatly affected by the climate, especially by irregular rainfall, the quantities of which vary from one year to

DOI: <http://dx.doi.org/10.25098/9.2.27>

another. A change is observed in the quantities of river water from one year to another, such that it is not stable even during one year. Also, the presence of quarries and continuous excavation work has led to an imbalance and lack of coordination between the movement of water in the river and the deposition of different soil particles.

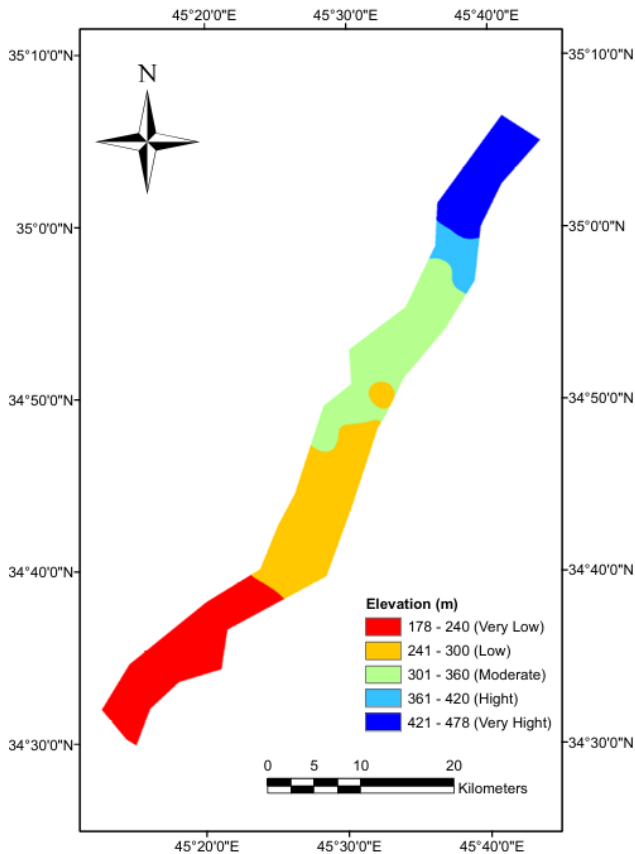


Figure 7: Elevation of the study area [Author]

4.3. Soil Texture Classification

The soil texture classes found in the study area are loamy and silty loam (Table 2 a, b and Figure 4, 5). The reason for the presence of these two classes and not the other texture classes is that the study area is the Sirwan River path and the majority of the soil texture in river path is silty because the silty texture is light enough to be carried by rivers for long distances and at the same time heavy enough to settle when the water speed slows down during the flow of water, sediments are sorted according to size and weight. Large particles such as sand are concentrated and settle first in the source or banks, while silt remains suspended in the water for longer distances and settles when the water flow slows down, for example in plains or during floods. Since sand is heavy, it settles quickly and does not travel long distances, while clay is very light, remaining suspended in water for long periods and only settles easily in still waters such as lakes. Therefore, silt is the ideal soil component for settling in medium- or low-velocity rivers. Generally, loamy and silty loam soil textures are found in rivers because they are medium-sized and are suited to the strength of river flow, so they are easily carried and settle at low velocities, while other textures do not have the same suitable conditions.

Through the soil texture classes in the study area (Figure 8), it is clear that the soil texture of the study area consists of loamy and silty loam soils, where the area occupied by the loamy soils is 106.42 km² of the total area of the study area, which conclude 66.51% of the total area of the study area. The loamy soil texture is a mixture of sand, silt and clay with an increase in the ratio of silt. As for the silty loam soil texture, its area is 53.58 km², which is a 33.49% of the total area of the study area. Through (Figure 8), it is clear that the loamy soil texture is concentrated at the ends of the study area, while the silty loam soil texture is concentrated in the middle of the study area. It is worth noting that this type of soil texture is considered one of the best soils for agriculture because it has good physical properties such as water retention and chemical properties such as increased fertility, it is also rich in organic matter.

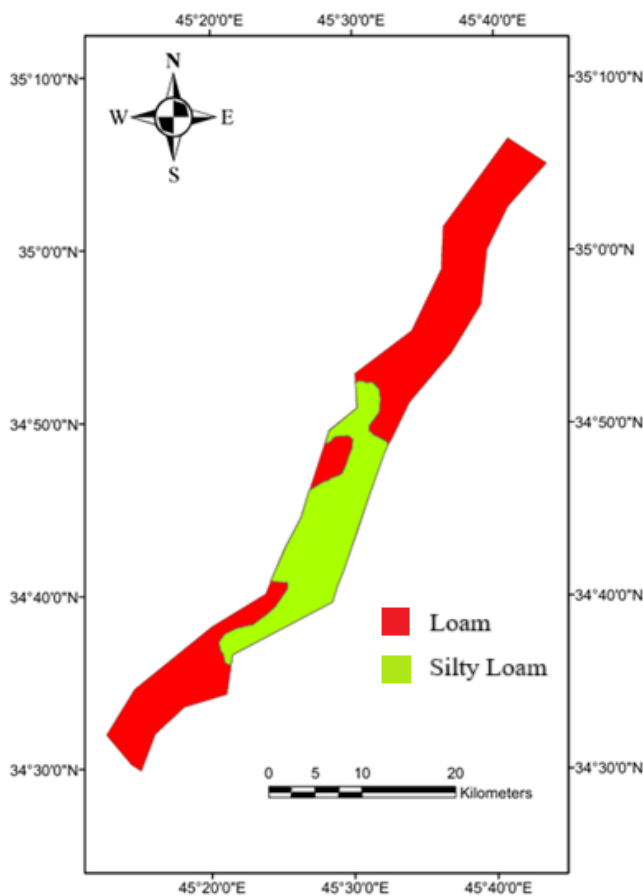


Figure 8: Soil texture classification in the study area [Author]

4.4. Statistical Analysis of Soil Particles

4.4.1. Left side

Figure 9, shown that the sand at the beginning of the river on the northern side is (318.41g/kg soil) then increases at its peak to 512.44 g/kg soil, then drops suddenly to reach (191.27 g/kg soil) in the middle of the river then increases in general gradually until it reaches (404.2 g/kg soil) at the end of the river. The silt is 463.79 g/kg soil at the beginning of the river, then it decreases slightly to 400.18 g/kg soil after that, it increases in the middle of the river to 557.51 g/kg soil, then at the end of the river it decreases again to be 480.79 g/kg soil. The dynamic movement of total clay is the opposite of silt, as it starts from 217.8 g/kg soil, then decreases to about 87.38 g/kg soil, then increases in the middle of the river to reach 266.32 g/kg soil, then decreases at the end of the river to 115.01 g/kg soil. The movement of fine clay is similar to the movement of total clay, as it starts from 104.3 g/kg soil, then decreases to 34.52 g/kg soil, then increases in the middle of the river to 143.48 g/kg soil, finally decreases in a fluctuating manner to finally stabilize at 28.53 g/kg soil.

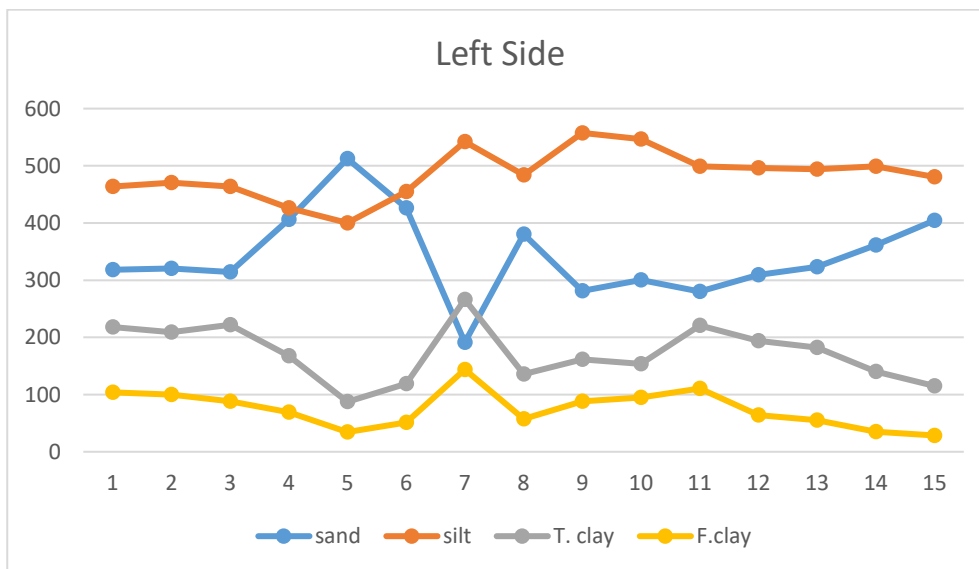


Figure 9: Chart diagram of soil particles of the left side of Sirwan River [Author]

Here are the Pearson correlation coefficients (R-values) between the variables:

Sand & Silt: -0.7996 → Strong negative correlation (as sand increases, silt decreases).

Sand & T. Clay: -0.8527 → Strong negative correlation (higher sand content is associated with lower total clay content).

Sand & F. Clay: -0.8212 → Strong negative correlation (similar to T. Clay).

Silt & T. Clay: 0.3681 → Moderate positive correlation.

Silt & F. Clay: 0.4702 → Moderate positive correlation.

T. Clay & F. Clay: 0.8624 → Strong positive correlation (more total clay means more fine clay).

Key Insights:

Sand content is inversely related to all other components.

Silt and clay components (T. Clay & F. Clay) have a positive relationship.

Fine clay (F. Clay) has a strong dependency on total clay (T. Clay).

4.4.2. Right Side

At the beginning of the river, the sand content is 331.38 g/kg soil, then decreases more steadily from the left side (Figure 10), then drops in the middle to 200.81 g/kg soil, and then gradually rises to 94.07 g/kg soil. The silt content starts at 441.8 g/kg soil, then rises steadily in the middle, unlike the left side, to reach 562.51 g/kg soil, and then decreases to stabilize at 466.17 g/kg soil. It is worth noting that the silt movement is opposite to that of the clay, up and down. On the other hand, total clay starts at 226.82 g/kg soil, fluctuates up and down, rising in the middle to 252.47 g/kg soil, then falling to 132.21 g/kg soil, rising again, then falling to 139.76 g/kg soil. It is noted from the movement of total clay that it is completely opposite to the movement of sand and parallel to the movement of silt. As for soft clay, the movement of soft clay is completely similar to the movement of total clay, starting at 109 g/kg soil, then fluctuating to reach 117.54 g/kg soil in the middle, then fluctuating up and down, falling and stabilizing at 29.87 g/kg soil.

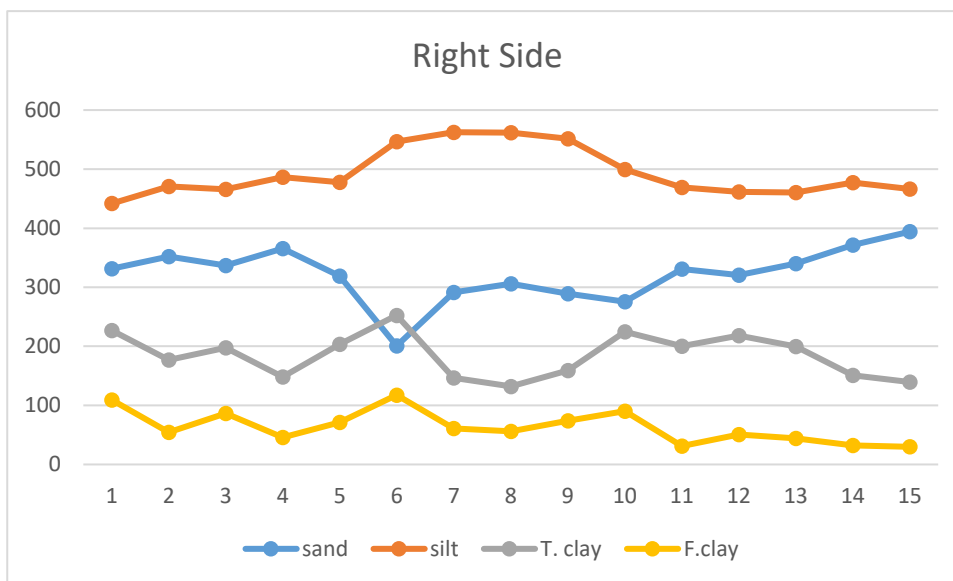


Figure 10: Chart diagram of soil particles of the right side of Sirwan River [Author]

Here are the Pearson correlation coefficients (R-values) between the variables:

Sand & Silt: -0.6439 → Moderate negative correlation.

Sand & T. Clay: -0.5374 → Moderate negative correlation.

Sand & F. Clay: -0.7179 → Strong negative correlation.

Silt & T. Clay: -0.2993 → Weak negative correlation.

Silt & F. Clay: 0.2195 → Weak positive correlation.

T. Clay & F. Clay: 0.6534 → Moderate-to-strong positive correlation.

Key insights:

Sand is inversely related to all other components, with a particularly strong negative correlation with F. Clay.

Silt and clay components (T. Clay & F. Clay) have a weak-to-moderate relationship.

T. Clay and F. Clay are positively correlated, meaning higher total clay content tends to include more fine clay.

In general, from diagrams one and two, it is noted that the movement of the particles and their quantities are more stable and less fluctuating on the right side. This is because the movement of the soil particles on the left side is more oscillating and more fluctuating due to the continuous change in the direction of the river on the left side. This is due to the abundance of gravel quarries where the excavation and transport mechanisms are constantly working in the excavation and transport operations of gravel and other soil materials.

The F.Clay/T.Clay index is an indicator of clay movement deep in the soil. The higher this percentage, the more fine clay there is at the expense of total clay. This indicates an increase in the surface area of the soil and, consequently, an increase in ionic exchange and soil fertility activity. On the other hand, the higher this percentage, the more soil development increases and developed horizons such as the Argillic horizon are formed and become thicker. In general, an increase in clay indicates an increase in soil activity, especially the movement of fine clay due to soil formation factors and processes. This is an indicator of the activity of pedological processes responsible for soil development, increased fertility and water retention. From (Figure 11), it is clear that the percentage of clay in the left-side is higher than the right-side of the river. This is evidence that the soil on the left-side is more developed than the right-side of the river in terms of soil formation and development.

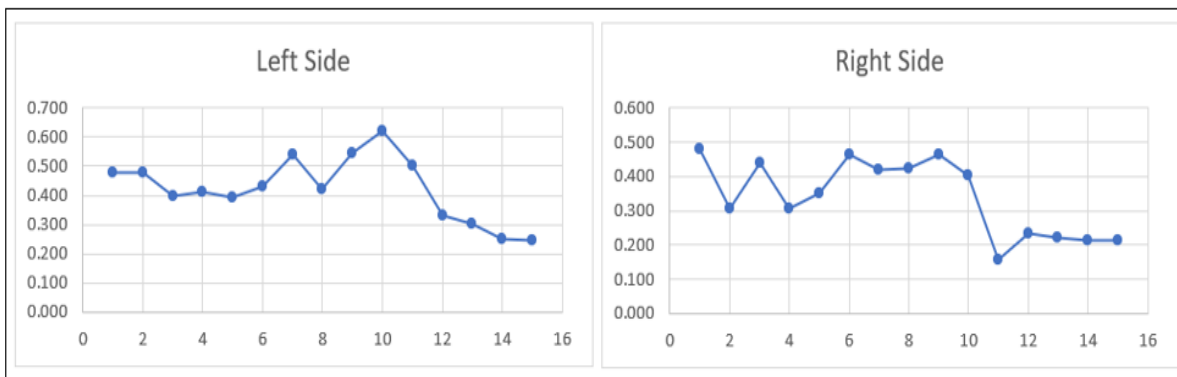


Figure 11: Indicator of F.Clay/T.Clay in both banks of Sirwan River [Author]

5. Conclusion and Recommendation

The soil texture along both banks of the Sirwan River in the Kurdistan Region of Iraq was successfully classified and analyzed in this research using a combination of remote sensing (RS) and geographic information system (GIS) approaches. To create complete maps showing the spatial distribution of sand, silt, clay, and fine clay, satellite data (Landsat 9) was combined with field sampling and laboratory analysis. The study region's soil texture classes were mainly loamy and silty loam, with loamy soils making up around 66.5% of the total 160 km² area and silty loam around 33.5%. The river's moderate flow rate makes the silty soils that predominate both banks perfect for sediment deposition. The right bank had a more uniform and stable soil distribution, while the left bank had a greater range of soil compositions and disruptions, which were probably caused by quarrying and changes in the river path. Clay fraction analysis revealed that the left bank soils are more developed, with a higher fine clay/total clay ratio, suggesting higher soil fertility and pedologic activity. The sedimentary sorting dynamics of riverine systems were supported by statistical connections between sand, silt, and clay, which revealed a clear inverse association between sand and the other elements. The application of RS and GIS made it possible to successfully model soil texture spatially, proving the value of these tools for monitoring the environment and planning agriculture.

The findings of this study have potential uses in soil conservation, land usage planning, and sustainable agriculture. The significance of high-resolution data is also highlighted, and the future integration of sophisticated technologies like hyperspectral imaging and unmanned aerial vehicles (UAVs) is suggested. The study ultimately offers helpful insights into the field of digital soil mapping and aids in making more informed decisions about the management of natural resources along changing river corridors. Finally, I recommend conducting further research in this field along river banks in the future, particularly using ground-based techniques, as they reduce the time, effort, and financial costs required to conduct this type of research. Riverbank areas are also particularly important for the agricultural sector, as the soil in these locations is characterized by high fertility and an ideal soil texture suitable for cultivation all types of crops.

References:

- [1] A. Irshad et al., “The role of water stress and soil texture on plant response in crop systems,” *Frontiers in Plant Science*, vol. 15, p. 1490001, 2024, [doi:10.3389/fpls.2024.1490001](https://doi.org/10.3389/fpls.2024.1490001).
- [2] I. Isaboke, O. Osano, O. S. Humphrey, et al., “Influence of Agricultural Land Use Management on Soil Particle Size Distribution and Nutrient Adsorption in Western Kenya,” *Chemistry Africa*, vol. 8, pp. 1599-1610, 2025, [doi:10.1007/s42250-025-01202-6](https://doi.org/10.1007/s42250-025-01202-6).
- [3] D. C. White, R. R. Morrison, P. A. Nelson et al., “Experimental Observations of Floodplain Vegetation, Bedforms, and Sediment Transport Interactions in a Meandering Channel,” *Journal of Geophysical Research: Earth Surface*, vol. 128, no. 9, 2023, [doi:10.1029/2023JF007136](https://doi.org/10.1029/2023JF007136).
- [4] J. Kadhim, M. Q. Waheed, H. A. Hussein, and S. F. A. Al-Wakel, “Experimental Study on the Effect of Flow Velocity and Slope on Stream Bank Stability (Part I),” *Civil Engineering Journal*, vol. 10, no. 8, p. 5080, 2024, [doi:10.28991/CEJ-2024-010-08-013](https://doi.org/10.28991/CEJ-2024-010-08-013).
- [5] A. G. Alghamdi, M. A. Majrashi, and H. M. Ibrahim, “Improving the Physical Properties and Water Retention of Sandy Soils by the Synergistic Utilization of Natural Clay Deposits and Wheat Straw,” *Sustainability*, vol. 16, no. 1, p. 46, Dec. 2023, [doi:10.3390/su16010046](https://doi.org/10.3390/su16010046).
- [6] F. Wang, P. Zhang, S. Chen, T. Shao, W. Lu, Z. Fang, C. Zhu, F. Liu, and J. Pan, “Spatial Prediction of Soil Texture in Low-Relief Agricultural Areas Using Rice and Wheat Growth Information with Spatiotemporal Stability,” *Remote Sensing*, vol. 17, no. 11, p. 1865, 2025, [doi:10.3390/rs17111865](https://doi.org/10.3390/rs17111865).
- [7] F. J. P. Wankmüller, L. Delval, P. Lehmann, M. J. Baur, A. Cecere, S. Wolf, D. Or, M. Javaux, and A. Carminati, “Global influence of soil texture on ecosystem water limitation,” *Nature*, vol. 635, no. 8039, pp. 631–638, Nov. 2024, [doi: 10.1038/s41586-024-08089-2](https://doi.org/10.1038/s41586-024-08089-2).
- [8] W. Abiye and O. Dengiz, “Digital mapping of soil erodibility factor in response to land use change using machine learning models,” *Environmental Systems Research*, vol. 14, no. 1, p. 14, 2025, [doi:10.1186/s40068-025-00402-w](https://doi.org/10.1186/s40068-025-00402-w).
- [9] C. A. U. Okeke, J. Uno, S. Academe, P. C. Emenike, T. K. S. Abam, and D. O. Omole, “An integrated assessment of land use impact, riparian vegetation and lithologic variation on streambank stability in a peri-urban watershed (Nigeria),” *Scientific Reports*, vol. 12, no. 1, Art. no. 10989, Jun. 2022, [doi: 10.1038/s41598-022-15008-w](https://doi.org/10.1038/s41598-022-15008-w).
- [10] R. Lu, H. He, A. Xie, X. He, C. Peng, Z. Li, and H. Zheng, “Seasonal variations in riverine sediment transport timescales in the Pearl River Estuary,” *Water*, vol. 17, no. 19, p. 2805, 2025, [doi:10.3390/w17192805](https://doi.org/10.3390/w17192805).
- [11] Q. Chen, E. Vaudour, and A. C. Richer-de-Forges, “Spectral indices in remote sensing of soil: definition, popularity, and issues,” *Remote Sensing of Environment*, vol. 329, p. 114918, 2025, [doi: 10.1016/j.rse.2025.114918](https://doi.org/10.1016/j.rse.2025.114918).
- [12] J. Shi, H. Yang, X. Hou, H. Zhang, G. Tang, H. Zhao, and F. Wang, “Coupling SAR and optical remote sensing data for soil moisture retrieval over dense vegetation covered areas,” *PLOS ONE*, vol. 20, no. 1, p. e0315971, 2025, [doi: 10.1371/journal.pone.0315971](https://doi.org/10.1371/journal.pone.0315971).
- [13] S. Dharumarajan, M. Lalitha, B. Kalaiselvi, S. Kaliraj, K. Adhikari, R. Vasundhara, K. V. Niranjana, et al., “Remote sensing of soils: Spectral signatures and spectral indices,” in *Remote Sensing of Soils*, Elsevier, 2024, pp. 13-23, [doi:10.1016/B978-0-12-824574-4.00002-5](https://doi.org/10.1016/B978-0-12-824574-4.00002-5).

- [14] Soil Survey Staff Keys to Soil Taxonomy, 13th ed.; U.S. Department of Agriculture, Natural Resources Conservation Service: Washington, DC, USA, 2022.
- [15] B. Chen, J. Wei, Q. Tang, Y. Gou, and C. Liu, "Estimating the Texture of Purple Soils Using Vis-NIR Spectroscopy and Optimized Conversion Models," *Agricultural Sciences*, vol. 14, no. 2, pp. 202–218, 2023, [doi:10.4236/as.2023.142014](https://doi.org/10.4236/as.2023.142014).
- [16] S. L. McGuirk and I. H. Cairns, "Relationships between Soil Moisture and Visible–NIR Soil Reflectance: A Review Presenting New Analyses and Data to Fill the Gaps," *Geotechnics*, vol. 4, no. 1, pp. 78-108, Jan. 2024, [doi: 10.3390/geotechnics4010005](https://doi.org/10.3390/geotechnics4010005).
- [17] F. Naz, M. Arif, T. Xue, and L. Changxiao, "Seasonal dynamics of soil ecosystems in the riparian zones of the Three Gorges Reservoir, China," *Global Ecology and Conservation*, vol. 54, p. e03174, 2024, [doi: 10.1016/j.gecco.2024.e03174](https://doi.org/10.1016/j.gecco.2024.e03174).
- [18] R. Mirzaeitarposhti, H. Shafizadeh-Moghadam, R. Taghizadeh-Mehrjardi, and M. S. Demyan, "Digital soil texture mapping and spatial transferability of machine learning models using Sentinel-1, Sentinel-2, and terrain-derived covariates," *Remote Sensing*, vol. 14, no. 23, p. 5909, 2022, [doi:10.3390/rs14235909](https://doi.org/10.3390/rs14235909).
- [19] J. J. Novais, M. P. C. Lacerda, E. E. Sano, J. A. M. Demattê, and M. P. Oliveira Jr., "Digital soil mapping using multispectral modeling with Landsat time series cloud computing based," *Remote Sensing*, vol. 13, no. 6, p. 1181, 2021, [doi:10.3390/rs13061181](https://doi.org/10.3390/rs13061181).
- [20] W. J. Wang, "Identification of soil texture and color using machine learning algorithms and satellite imagery," *Scientific Reports*, vol. 15, no. 1, Art. no. 30982, 2025, [doi:10.1038/s41598-025-17166-z](https://doi.org/10.1038/s41598-025-17166-z).
- [21] S. Miletić, J. Beloica, and P. Miljković, "Integrating Environmental Variables into Geostatistical Interpolation: Enhancing Soil Mapping for the MEDALUS Model in Montenegro," *Land*, vol. 14, no. 4, p. 702, 2025, [doi:10.3390/land14040702](https://doi.org/10.3390/land14040702).
- [22] S. M. Balaky, G. F. Hassan, A. O. Hussein, B. A. Delizy, and I. S. Asaad, "Facies association and depositional environment of the Sarmord Formation (Valanginian-Aptian), Kurdistan Region, Northeastern Iraq," *Iraqi Geological Journal*, vol. 56, no. 2F, pp. 132–147, 2023, [doi: 10.46717/igj.56.2F.9](https://doi.org/10.46717/igj.56.2F.9).
- [23] K. D. Muslih and A. M. Abbas, "Climate of Iraq," in *The Geography of Iraq*, Cham: Springer Nature Switzerland, 2024, pp. 19–47. [doi: 10.1007/978-3-031-71356-9](https://doi.org/10.1007/978-3-031-71356-9).
- [24] S. N. Azeez, "Effects of some local conditions on leaching factor of Aridisols in Kalar/Garmian, Kurdistan-Iraq," *Kurdistan Journal of Applied Research (KJAR)*, vol. 1, no. 2, 2016. [Online]. Available: <http://kjar.spu.edu.iq>. <https://doi.org/10.24017/science.2016.1.2.1>
- [25] S. N. Azeez, "Classification of Serwan river levee's soils in Kurdistan Region-Iraq," *Journal of Garmian University*, vol. 4, no. 4, 2017. [Online]. Available: <http://jgu.garmian.edu.krd>. [doi: 10.24271/garmian.217](https://doi.org/10.24271/garmian.217)
- [26] S. N. Azeez, "Mapping of total lime using remote sensing and GIS technology, case study: Garmian District, Kurdistan Region-Iraq," *Passer Journal*, vol. 5, no. 2, pp. 143–248, 2023. [Online]. Available: <http://passer.garmian.edu.krd/>. [DOI: 10.24271/PSR.2023.387488.1266](https://doi.org/10.24271/PSR.2023.387488.1266).
- [27] J. K. Kassim, K. Z. Al-Janabi, and M. I. Karim, "Soil temperature regimes in Iraq: II – Relationship between soil temperature and latitude, longitude and elevation," *Journal of Agriculture and Water Resources Research*, vol. 8, no. 1, pp. 111–121, 1989.

- [28] F. H. Al-Taie, C. Sycand, and G. Stoops, "Soil groups of Iraq, their classification and characteristics," *Pedologie*, no. 19, pp. 65–148, 1969.
- [29] Food and Agriculture Organization (FAO) of the United Nations, *Agriculture Pest and Their Control Principles*. Erbil, Iraq: Offset Press, 2000.
- [30] S. M. Ahmad, Natural Map of Iraqi Kurdistan Region. 2005.
- [31] F. H. Al-Taie, The Soils of Iraq, Ph.D. dissertation, State Univ. of Ghent, Ghent, Belgium, 1968.
- [32] Soil Survey Staff, *Keys to Soil Taxonomy*, 12th ed., USDA Natural Resources Conservation Service, Washington, DC, 2014.
- [33] V. J. Kilmer and L. T. Alexander, "Methods of making mechanical analysis of soils," *Soil Sci.*, vol. 68, pp. 15–24, 1949.
- [34] M. L. Jackson, *Soil Chemical Analysis: Advanced Course — A Manual of Methods*, Revised ed. Roorkee, India: Scientific Publishers / United Book Prints, 2017. ISBN 978-9383692354.
- [35] M. L. Jackson, *Soil Chemical Analysis: Advanced Course*, 2nd ed. Madison, WI, USA: Published by the author, 1979.
- [36] Soil Survey Staff, *Kellogg Soil Survey Laboratory Methods Manual*, Soil Survey Investigations Report No. 42, Version 6.0, U.S. Department of Agriculture, Natural Resources Conservation Service, 2023. Available at: <https://www.nrcs.usda.gov/sites/default/files/2023-01/SSIR42>
- [37] C. Ditzler, K. Scheffe, and H. C. Monger, *Soil Survey Manual*, USDA Handbook 18, 2017.
- [38] K. Lulla, M. D. Nellis, B. Rundquist, P. K. Srivastava, and S. Szabo, "Mission to earth: LANDSAT 9 will continue to view the world," *Geocarto Int.*, vol. 36, no. 20, pp. 2261–2263, 2021. <https://doi.org/10.1080/10106049.2021.1991634>.